PRIMARY NEBULAR SULFIDES IN CR AND CM CHONDRITES: FORMATION BY SULFIDIZATION AND CRYSTALLIZATION. S. A. Singerling and A. J. Brearley, Department of Earth and Planetary Sciences, MSC03-2040, 1 University of New Mexico, Albuquerque, NM 87131. Email: ssingerling@unm.edu.

Introduction: Distinguishing primary solar nebular features in chondritic meteorites from those resulting from secondary processes on asteroidal parent bodies is essential in determining the conditions present in these two different environments. Mineral grains that formed from direct condensation of nebular gas are primary grains in the strictest sense. However, we consider primary grains to be anything that formed in the solar nebula either by condensation, reaction of condensates with a nebular gas, or by the melting of condensates by thermal events in the nebula.

Iron sulfides could have formed in the solar nebula from reactions between condensate Fe,Ni-metal with nebular gas (H_2S, specifically). This reaction yields the monosulfide solid solution (mss, $(Fe,Ni)_{1-x}S$):

Fe,Ni-metal (s) + H_2S (g) = $(Fe,Ni)_{1-x}S$ (s)

Monosulfide solid solution is not stable at temperatures below ~610°C [1] and begins to unmix into pyrrhotite ($Fe_{1-x}S$) and pentlandite ($(Fe,Ni)_9S_8$) yielding pyrrhotite-pentlandite (po-pn) exsolution textures.

Primary sulfides are also likely to have formed during the chondrule-forming flash heating event [2-4]. In this scenario, flash heating resulted in partial to complete melting of preexisting grains. Cooling below 610°C resulted in crystallization of sulfide melts and subsolidus unmixing yielding po-pn exsolution textures.

Chondritic primary sulfides may have formed from 1) sulfidization and/or 2) crystallization from sulfide melts. The formation of po-pn exsolution textures depends on temperature and Ni-content of the sulfide. Because metal diffusion rates in sulfides are rapid, thermal metamorphism is likely to obliterate exsolution textures. For this reason, we restricted our studies to low petrologic type chondrites (<3.00). CR and CM carbonaceous chondrites are ideal as both groups are predominantly petrologic type 2, having experienced aqueous alteration, but not thermal metamorphism [5]. Several workers [6, 7] propose that secondary sulfides, formed from interaction of primary sulfides or metals with water on asteroidal parent bodies, are also present in CR and CM chondrites. This subject is an area of future work and will not be treated here.

Previous work has identified sulfides that may have formed from both sulfidization [8] and crystallization [3, 4, 9, 10]. Our work involves reevaluating the sulfide mineralogy of the CR and CM carbonaceous chondrites to determine if primary sulfides that formed from sulfidization and/or crystallization are present within chondrules, and if so, what these grains can tell us about nebular conditions during their formation.

Methods: The meteorites studied for this work include: CR2s QUE 99177, EET 92042, and MET 00426 and CM2s QUE 97990, Murchison, Murray, and Mighei. BSE images were obtained on a FEI Quanta 3D FEGSEM in the E&PS Dept. at UNM. WDS compositional data of sulfides were collected using a JEOL 8200 EPMA and Probe for EPMA (PFE) software in the Institute of Meteoritics at UNM.

Results: The coarse-grained (>10 μm) sulfides in CRs are present as isolated grains in the matrix, in the less abundant type IIA (FeO-rich) chondrules, and in type IA (FeO-poor) chondrules. In CMs, they are present in the matrix, in type IIA chondrules, and less commonly, in type IA chondrules. The majority of the grains in both meteorite groups are 20-30 μm in size and spherical to subhedral to anhedral. Two textural groups were observed and include sulfide rimmed metal (SRM) grains and po-pn composite (COMP) grains. Overall, the COMP grains are much more common in both CRs and CMs.

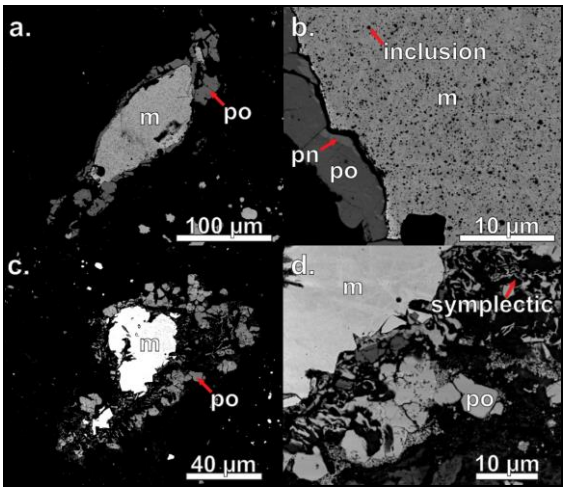

Fig. 1. BSE images of SRM grains in (a & b) CR2 EET 92042 and (c & d) CM2 QUE 97990. CR: clean boundaries between metal and sulfide and C-bearing inclusions in metal in (b). CM: complex boundaries between metal and sulfide (symplectic texture) in (d). po = pyrrhotite, pn = pentlandite, m = metal.

The SRM grains (Fig. 1) are characterized by an Fe,Ni-metal core rimmed by sulfide displaying po-pn exsolution. For a more comprehensive explanation of po-pn exsolution textures, see [10]. Most of the SRM grains in the CRs have thin sulfide rims (5-10 μm) around metals in type IA chondrules. An exception occurs in an intermediate type chondrule (between IA and IIA) in EET 92042, which has thicker sulfide rims (up to 50 μm). The po-pn exsolution features are, con-

sequently, easier to discern and include pn patches, blades, and rods (Fig. 1b). The metal in these SRM grains contains submicron-sized inclusions of a C-bearing phase (Fig. 1b) as determined using EDS.

SRMs in CMs are very rare and have only been observed in the matrix. An example from QUE 97990 is shown in Fig. 1c-d. The contact between the metal and sulfide is complex with a silicate-sulfide symplectitic texture (Fig. 1d). The sulfide rim is composed mostly of granoblastic polygonal po showing corrosion. Pentlandite patches and the snowflake exsolution texture (of [10] and first observed by [11]), an inverse texture with lesser amounts of po occurring as dendritic to graphic growths in pn patches, are present in the po surrounding the metal.

The COMP grains (Fig. 2) are dominated by po with lesser amounts of pn occurring as patches, blades, lamellae, and submicron rods. The snowflake texture is commonly observed. A small subset of the COMP grains also contain micron-sized metal inclusions (MMIs) as depicted in Fig. 2e. The majority of the MMIs are located in po and have blades of pn nucleating off of them. A few MMIs in CRs are located within pn patches. MMIs have previously been identified by [8] and [10]. The COMP grains are similar in both CRs and CMs.

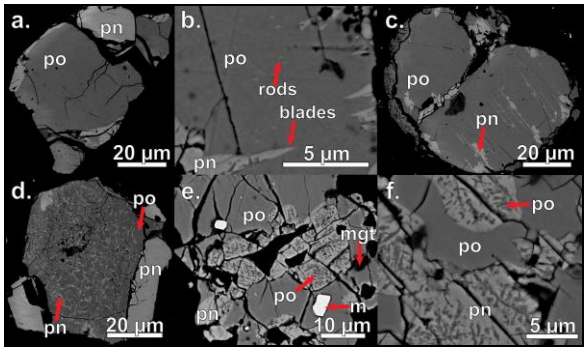

Fig. 2. BSE images of COMP grains from CM2 QUE 97990. (a) pn patches, (b) submicron rods of pn and pn blades, (c) irregular pn lamellae, (d) pn patches and pn crossed lamellae, (e) snowflake texture and MMI, and (f) snowflake texture. po = pyrrhotite, pn = pentlandite, m = metal, mgt = magnetite.

Compositional data for SRM grains, COMP grains, and MMIs are presented in Fig. 3. The SRM analyses are average values for each phase from multiple probe points. The COMP grain analyses are presented as bulk compositions determined using modal recombination analysis [after 12]. The MMIs are average values from multiple analyses of the same grain. The MMI data were corrected for secondary fluorescence effects using PENEPMA in PFE due to the small sizes of the inclusions (1-6 µm).

Discussion: The SRM grains likely formed by sulfidization in the solar nebula as they have the appropriate morphology [14] and contain metal with the solar Co/Ni ratio (0.045 from [13]). The COMP grains likely formed by crystallization within chondrules as many are present within chondrules and display po-pn exsolution consistent with experimental work cooling mss from high temperatures (~800°C) [15-17].

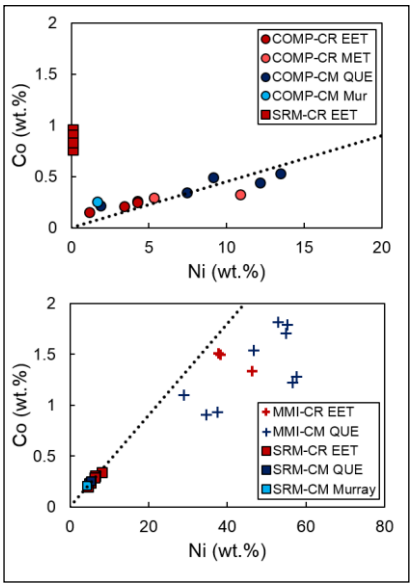

Fig. 3. Element-element diagrams for sulfide (top) and metal (bottom) EPMA analyses. Colors correspond to samples (reds = CRs, blues = CMs). Symbols correspond to textural group (circle = COMP, square = SRM, cross = MMIs). The dashed line represents the solar Co/Ni ratio [from 13].

The MMIs may be relicts of incomplete sulfidization of metal grains as similar Ni-rich metals were produced by [14] in experimental work. In this case, the metal compositions changed from the solar Co/Ni ratio as a result of resorption and differential partitioning of Co and Ni between sulfide and metal as the metal was consumed. The presence of MMIs in COMP grains, however, argues for an alternative explanation. They may instead have formed from a melt that lost sulfur by evaporation during chondrule melting. In this case, the melt was enriched in metal atoms relative to the stoichometry of mss and crystallized Fe,Ni-metal grains during cooling. [18] have proposed a similar explanation for the formation of metal inclusions in troilite from chassignite NWA 2737.

Acknowledgements: This work was supported by NASA Cosmochemistry grant NNX11AK51G to AJ Brearley (PI).

References: [1] Kerridge J. F. et al. (1979) *EPSL*, *43*, 359-67. [2] Boctor N. Z. et al. (2002) *LPS XXXIII*, Abstract #1534. [3] Brearley A. J. and Martinez C. (2010) *LPS XLIII*, Abstract #1438. [4] Harries D. and Langenhorst F. (2013) *MAPS*, *48*, 879-903. [5] Wood J. A. (1962) *GCA*, *26*, 739-49. [6] Fuchs L. H. et al. (1973) *Sm. Contr. Earth Sci.*, *10*, 1-39. [7] Bullock E. S. et al. (2007) *LPS XXXVIII*, Abstract #2057. [8] Schrader D. L. et al. (2008) *GCA*, *72*, 6124-40. [9] Maldonado E. M. and Brearley A. J. (2011) *LPS XLII*, Abstract #2271. [10] Singerling S. A. and Brearley A. J. (2014) *LPS XLV*, Abstract #2132. [11] Brearley A. J. (2010) *73rd Met. Soc.*, Abstract #5159. [12] Berlin J. (2009) *Ph.D. Thesis, UNM*. [13] Anders E. and Grevesse N. (1989) *GCA*, *51*, 197-214. [14] Schrader D. L. and Lauretta D. S. (2010) *GCA*, *74*, 1719-33. [15] Misra K. C. and Fleet M. E. (1973) *Econ. Geol. 68*, 518-39. [16] Durazzo A. and Taylor L. A. (1982) *Min. Dep.*, *17*, 313-32 [17] Estchmann B. et al. (2004) *Am. Min. 89*, 39-50. [18] Lorand J.-P. et al. (2012) *MAPS*, *47*, 1830-41.